Am J Cancer Res 2024;14(4):1712-1729
www.ajcr.us /ISSN:2156-6976/ajcr0155418

Original Article

A signature of seven hypoxia-related lncRNAs is a potential biomarker for predicting the prognosis of melanoma

Yunyang Wu[1,2*], Shenhui Yin[3*], Chunzhen Li[3], Liyuan Zhao[3], Mengqi Song[3], Yizhi Yu[3], Ling Tang[1,2], Yanlong Yang[1,2]

[1]School of Traditional Chinese Medicine, Naval Medical University, Shanghai, China; [2]Department of Traditional Chinese Medicine, The First Affiliated Hospital of Naval Medical University, Shanghai, China; [3]National Key Laboratory of Immunity & Inflammation, Naval Medical University, Shanghai, China. [*]Equal contributors.

Received January 12, 2024; Accepted April 9, 2024; Epub April 15, 2024; Published April 30, 2024

Abstract: Melanoma is the most aggressive type of skin cancer and has a high mortality rate once metastasis occurs. Hypoxia is a universal characteristic of the microenvironment of cancer and a driver of melanoma progression. In recent years, long noncoding RNAs (lncRNAs) have attracted widespread attention in oncology research. In this study, screening was performed and revealed seven hypoxia-related lncRNAs AC008687.3, AC009495.1, AC245128.3, AL512363.1, LINC00518, LINC02416 and MCCC1-AS1 as predictive biomarkers. A predictive risk model was constructed via univariate Cox regression analysis, least absolute shrinkage and selection operator (LASSO), and multivariate Cox regression analyses. Patients were grouped according to the model risk score, and Kaplan-Meier analysis was performed to compare survival between groups. Functional and pathway enrichment analyses were performed to compare gene set enrichment between groups. Moreover, a nomogram was constructed with the risk score as a variable. In both the training and validation sets, patients in the low-risk group had better overall survival than did those in the high-risk group ($P<0.001$). The 3-, 5- and 10-year area under the curve (AUC) values for the nomogram model were 0.821, 0.795 and 0.820, respectively. Analyses of immune checkpoints, immunotherapy response, drug sensitivity, and mutation landscape were also performed. The results suggested that the low-risk group had a better response to immunotherapeutic. In addition, the nomogram can effectively predict the prognosis and immunotherapy response of melanoma patients. The signature of seven hypoxia-related lncRNAs showed great potential value as an immunotherapy response biomarker, and these lncRNAs might be treatment targets for melanoma patients.

Keywords: Hypoxia-related lncRNAs, potential biomarker, melanoma

Introduction

Melanoma, an extremely aggressive skin cancer with a high metastasis rate, is a significant threat to human health. Patients with metastasis generally have a poor prognosis [1, 2]. In 2020, there were 32385 and 24658 melanoma-related deaths in males and females, respectively; the age-standardized incidence rates were 0.7 and 0.4, and the cumulative risks of developing melanoma were 0.07%, and 0.05%, respectively [3]. Moreover, the incidence, mortality, and disability-adjusted life years (DALYs) of melanoma have increased dramatically [4]. In the past decade, the survival rate of patients with metastatic melanoma has significantly improved due to the development of a combination of targeted therapies and immune checkpoint inhibitors [5]. However, in the later stage of treatment, many patients present with disease recurrence, drug resistance, and accelerated melanoma progression. According to previous reports, approximately 40-65% and 70% of patients acquire resistance to immune checkpoint inhibitors targeting programmed cell death protein 1 (PD-1) and cytotoxic T lymphocyte antigen-4 (CTL-4), respectively [6]. Therefore, exploring more effective biomarkers for future therapeutic interventions for melanoma patients is imperative.

Long noncoding RNAs (lncRNAs), as significant modulators of tumorigenesis, have received extensive attention in recent years [7, 8]. LncRNAs, a class of RNA transcripts with a length greater than 200 nucleotides, can affect various biological behaviors, such as cell proliferation, invasion, and metastasis in skin cancers. Xu et al. reported that lncRNAs related to "evading immune destruction" can predict the response to anti-PD-1 immunotherapy [9]. The lncRNA KCNQ1OT1 can promote immune evasion of melanoma cells via the miR-34a/STAT3/PD-L1 axis [10]. LINC00632 can cause cerebellar degeneration-related 1 antisense depletion through epigenetic silencing, promoting the invasion and metastasis of melanoma [11]. Furthermore, lncRNAs play a critical role in melanoma diagnosis and prognosis evaluation [12]. The expression of the lncRNA BASP1-AS1 can promote the malignancy of melanoma [13]. Overexpression of the long noncoding RNA NORAD promotes the migration and invasion of malignant melanoma cells [14].

The tumor microenvironment (TME) is usually in a hypoxia state. Numerous studies have revealed that the hypoxic microenvironment is essential for melanoma progression. Hypoxia can promote melanoma progression and resistance to therapy [15]. For example, hypoxia-inducible factor-1 (HIF-1) is a critical transcriptional regulator in the hypoxic tumor microenvironment; it induces the expression of immunosuppressive factors and immune checkpoint molecules. HIF-1 is involved in multiple signaling pathways and has been implicated in angiogenesis, metabolism, cell proliferation, and metastasis in melanoma [16, 17]. According to previous hypoxia-related predictive models for melanoma, the analysis of the predictive power of these models was mainly focused on the time points of 1, 3, and 5 years, and the predictive power of the nomogram was limited [18, 19]. Therefore, an in-depth analysis of hypoxia-related lncRNAs is a viable method for identifying potential melanoma interventions. In this study, we obtained expression data from the University of California Santa Cruz (UCSC) Xena database to comprehensively explore the critical prognostic role of hypoxia-related lncRNAs in melanoma. A prognostic model of seven hypoxia-related lncRNAs was established. The prognostic value of the model was then assessed in the training and validation cohorts. Moreover, we explored the underlying biological functions of these hypoxia-related lncRNAs. Ours model can aid in melanoma prognosis prediction and provides new biomarkers that might be treatment targets for melanoma in the future.

Materials and methods

Data collection and preprocessing

The RNA-sequencing data and corresponding clinical information on patients with melanoma were obtained from The Cancer Genome Atlas (TCGA) database via the University of California Santa Cruz (UCSC) Xena browser (http://xena.ucsc.edu/). The TCGA database contained information on 471 melanoma tumor samples and one adjacent normal sample. The gene expression profiles of 812 normal skin samples were downloaded from the Genotype-Tissue Expression (GTEx) database to increase the sample size for the normal sample group. The mutation profiles of all tumor samples were obtained from the TCGA database.

Identification of hypoxia-related lncRNAs for prognosis prediction

Hypoxia-related genes in the HALLMARK_HYPOXIA (M5891) gene set were downloaded from the Molecular Signatures Database v7.5 (MSigDB) (https://www.gsea-msigdb.org). The gene annotation files were downloaded from the Ensembl database (http://www.ensembl.org) for separating the genes into messenger RNAs (mRNAs) and lncRNAs for subsequent analyses. A |correlation coefficients| >0.5 and a p-value <0.001 were considered to indicate hypoxia-related lncRNAs. LncRNAs and hypoxia-related genes with average expression levels less than 0.1 and 0.5, respectively, were excluded. The Wilcoxon test was used to analyze the differential expression of hypoxia-related lncRNAs between tumor and normal tissue samples in the TCGA and Genotype-Tissue Expression (GTEx) datasets. LncRNAs with an FDR<0.05 and an absolute log-fold change >1 were defined as differentially expressed lncRNAs. Moreover, we used the R package "caret" to randomize melanoma patients into training and testing cohorts at a 7:3 ratio.

Development and identification of a hypoxia-related lncRNA prognostic signature

Univariate Cox proportional hazard regression, LASSO regression, and stepwise multivariate Cox regression analyses were performed to identify the best prognostic hypoxia-related lncRNAs in the training set; these analyses were performed by using the "glmnet" and "survival" packages in R. The risk score was calculated using the following formula: risk score = $\sum_i^n coefIncRNAi * expIncRNAi$ (coefIncRNAi: the coefficient of hypoxia-lncRNAi, expIncRNAi: the expression levels of hypoxia-related lncRNAi).

The training, testing and entire cohorts were divided into high and low-risk groups according to the median risk score in the training set. Kaplan-Meier survival curves were drawn using the "survival" and "survminer" R packages. Moreover, we used the "survivalROC" R package to verify the accuracy of the prognostic model according to the time-dependent receiver operating characteristic (ROC) curves for 3-, 5- and 10-year survival. Univariate and multivariate Cox regression analyses were used to evaluate the independent prognostic value of the signature.

Nomogram construction and validation

Based on the univariate and multivariate analysis results, independent prognostic factors affecting overall survival (OS) were included in the constructed nomogram using the "rms" R package. Calibration and decision curve analyses were applied to evaluate the calibration and discrimination ability of the nomogram.

Functional and pathway enrichment analysis

Consistent with the previous analysis, an FDR<0.05 and a log-fold change >1 were used to define the differentially expressed lncRNAs between the two risk groups. Gene Ontology (GO) and Kyoto Encyclopedia of Genes and Genomes (KEGG) analyses of the differentially expressed lncRNAs between the two risk groups were performed with the "org.Hs.eg.db", "clusterProfiler", "ggplot2" and "enrichplot" R packages. The enrichment of differentially expressed genes between the two risk subgroups in the HALLMARK gene sets was analyzed via gene set enrichment analysis (GSEA) software (version 4.2.3). NOM *p*-value <0.05, |NES|>1.0, and FDR<0.25 indicated statistical significance.

Immune cell infiltration and tumor microenvironment analysis

Information for estimating immune cell infiltration for TCGA tumors was downloaded from the TIMER website (http://timer.cistrome.org/). Single-sample gene set enrichment analysis (ssGSEA) and the CIBERSORT algorithm were used to assess the status of immune cell infiltration in melanoma. The CIBERSORT algorithm was used to assess the level of infiltration of 22 immune cell subtypes [20]. The annotated gene signatures of 22 immune cell subtypes were obtained from the CIBERSORT website (https://cibersort.stanford.edu/). The immune cell gene sets used in the ssGSEA were downloaded from the TISIDB website and included 28 tumor-infiltrating lymphocyte (TIL) gene signatures. The stromal score, immune score, ESTIMATE score, and tumor purity were assessed using the "estimate" R package [21].

Association of immune checkpoint expression, immunotherapy response, and immunophenoscore (IPS) with the prognostic signature

The advent of immune checkpoint inhibitors has significantly improved survival rates in patients with metastatic melanoma [22]. We analyzed the expression of immune checkpoint genes reported by Hu et al. [23]. In addition, the five common immune checkpoint genes (CD274, PDCD1, CTLA4, LAG3, and HAVCR2) were found to be clearly correlated with the risk score. The five immune checkpoint genes were also chosen based on previous reports [24]. The immunotherapy response data were obtained from an online website (http://bioinfo.life.hust.edu.cn/ImmuCellAI#!/). The IPS data of The Cancer Genome Atlas-Skin Cutaneous Melanoma (TCGA-SKCM) cohort were downloaded from The Cancer Immunome Atlas (TCIA) (https://tcia.at/home).

Chemotherapeutic drug sensitivity and gene mutation analysis

The "oncoPredict" package of R was used to predict the clinical drug response for many cancer drugs [25]. The 50% maximum inhibitory concentration (IC50) was used as the outcome variable. The drug IC50s of the two risk sub-

groups were compared by the Wilcoxon signed rank test. The frequency and type of gene mutations in risk subgroups from the cBioPortal database were assessed using the "Maftools" R package. The differences in tumor mutation burden (TMB) scores between the high- and low-risk groups were also assessed via the Wilcoxon signed-rank test.

Statistical analysis

All the statistical data were analyzed with R software (version 4.2.3). A chi-square test was used to analyze the differences in clinicopathological characteristics between the training and testing sets. The Mann-Whitney U test was used to analyze the survival time of patients in the different cohorts. The Kaplan-Meier method was used to evaluate the survival curves, and the log-rank test was used to assess the significance of any differences in survival [26]. The correlation between the expression of the seven hypoxia-related lncRNAs and immune cells was assessed via Spearman correlation analysis. The Delong test was used to compare the AUCs between the training and testing cohort. For all the statistical analyses, $P<0.05$ was considered to indicate statistical significance (*P<0.05, **P<0.01, ***P<0.001).

Results

Data preprocessing and identification of hypoxia-related lncRNAs in melanoma

The workflow of the study is shown in **Figure 1**. In the TCGA dataset, patients with insufficient clinical data for variables such as age; sex; pathologic stage; tumor (T), node (N), and metastasis (M) stage; survival time; and outcome or those with OS less than 90 days were excluded from the study. Finally, 408 patients were enrolled. There were no differences ($P>0.05$) in clinical characteristics between the training and testing cohorts (**Table 1**). To explore hypoxia-related lncRNAs in melanoma, we analyzed the correlation between hypoxia-related genes and lncRNAs using $P<0.001$ and $|Cor|>0.5$ as the cutoff. A total of 421 hypoxia-related lncRNAs were identified. A total of 249 hypoxia-related lncRNAs were screened as differentially expressed hypoxia-related lncRNAs by the Wilcoxon test (**Figure 2A**).

Construction and internal validation of the hypoxia-related lncRNA prognostic signature

Before constructing the hypoxia-related lncRNA predictive model, we integrated the lncRNA expression data and clinical information. Patients without complete lncRNA expression data were excluded. According to the univariate Cox regression analyses, 125 lncRNAs were significantly related to OS. Subsequently, we performed a LASSO regression analysis and identified 13 prognostic lncRNAs (**Figure 2B**, **2C**). Finally, using multivariate stepwise Cox regression (**Figure 2D**), seven hypoxia-related lncRNAs with better prognostic value were identified to establish a prediction model. The expression of seven hypoxia-related lncRNAs in the normal and tumor samples in TCGA and GTEx databases are shown in Supplementary Figure 1. The interaction network and Sankey diagram showed the associations of the hypoxia-related genes with the seven hypoxia-related lncRNAs (**Figure 2E**, **2F**). The correlation coefficients and expression level of seven hypoxia-related lncRNAs were used to calculate the risk score. The formula was as follows:

Riskscore = AC008687.3 × (4.604700878) + AC009495.1 × (0.197320671) + AC245128.3 × (-0.33477854) + AL512363.1 × (0.577976475) + LINC00518 × (0.086438824) + LINC02416 × (-0.64361001) + MCCC1-AS1 × (-0.80139977).

Based on the median risk score of the training set, all patients in the training, testing, and entire cohorts were classified into high and low-risk groups. Risk scores and survival status of patients and expression of the seven hypoxia-related lncRNAs in different risk groups were shown in **Figure 3A-C**. Kaplan-Meier curves demonstrated that patients in the high-risk group had worse OS than did patients in the low-risk group in the training cohort (**Figure 3D**). Similar results were also verified in the testing cohort (**Figure 3E**) and entire cohort (**Figure 3F**). The time-dependent ROC curves indicated that the risk model had excellent prognostic accuracy and stability. The AUC values in the training cohort at 3-, 5- and 10-year were 0.734, 0.738, and 0.741, respectively (**Figure 3G**). The AUC values for 3-, 5-, and 10-year were 0.640, 0.672, and 0.769, respectively, in the testing cohort (**Figure 3H**) and 0.708, 0.723,

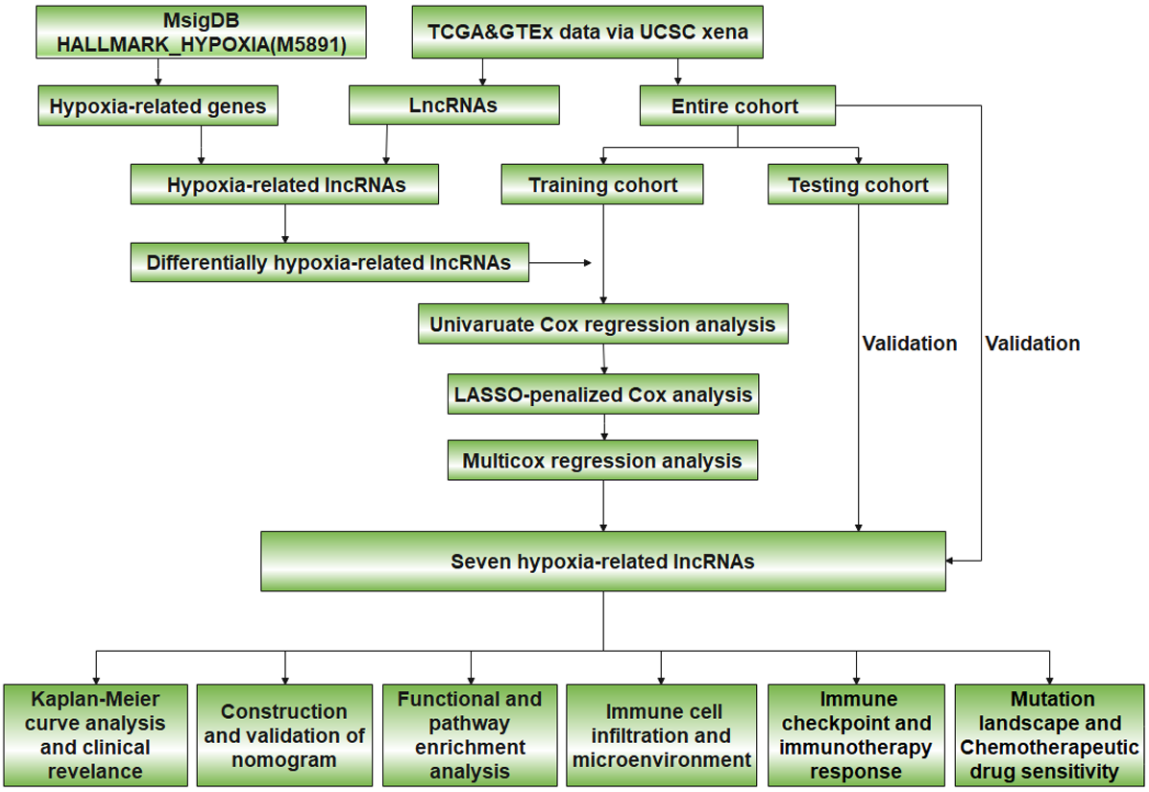

Figure 1. Flow chart of this study.

Table 1. Clinical characteristics of the training cohort and the testing cohort

Variables	Group	Entire cohort (n=408)	Training cohort (n=286)	Testing cohort (n=122)	*p*-value
Age	≥65	147 (36.0%)	98 (34.3%)	49 (40.2%)	0.306
	<65	261 (64.0%)	188 (65.7%)	73 (59.8%)	
Gender	Female	151 (37.0%)	111 (38.8%)	40 (32.8%)	0.297
	Male	257 (63.0%)	175 (61.2%)	82 (67.2%)	
Vital status	Alive	207 (50.7%)	148 (51.7%)	59 (48.4%)	0.604
	Dead	201 (49.3%)	138 (48.3%)	63 (51.6%)	
Stage	I/II nos	10 (2.5%)	7 (2.4%)	3 (2.5%)	0.847
	Stage 0	6 (1.5%)	4 (1.4%)	2 (1.6%)	
	Stage I	77 (18.9%)	56 (19.6%)	21 (17.2%)	
	Stage II	128 (31.4%)	91 (31.8%)	37 (30.3%)	
	Stage III	167 (40.9%)	112 (39.2%)	55 (45.1%)	
	Stage IV	20 (4.9%)	16 (5.6%)	4 (3.3%)	
Survival time (days)		1116.5 (518.25, 2366.5)	1146 (552, 2375.75)	919 (484.25, 2375)	-0.621

and 0.753 in the entire cohort (**Figure 3I**). Furthermore, we used the Delong test to compare the AUC of the training and testing cohorts. There is no significant difference between the training set and validation set in terms of predictive ability at 3, 5 and 10 years (Delong test, P>0.05). The results of the Kaplan-Meier curve analysis also showed that OS was significantly longer in the low-risk group. The seven hypoxia-related lncRNAs exhibited the same expression trends in the training and two validation cohorts. The expression levels of AL512373.1,

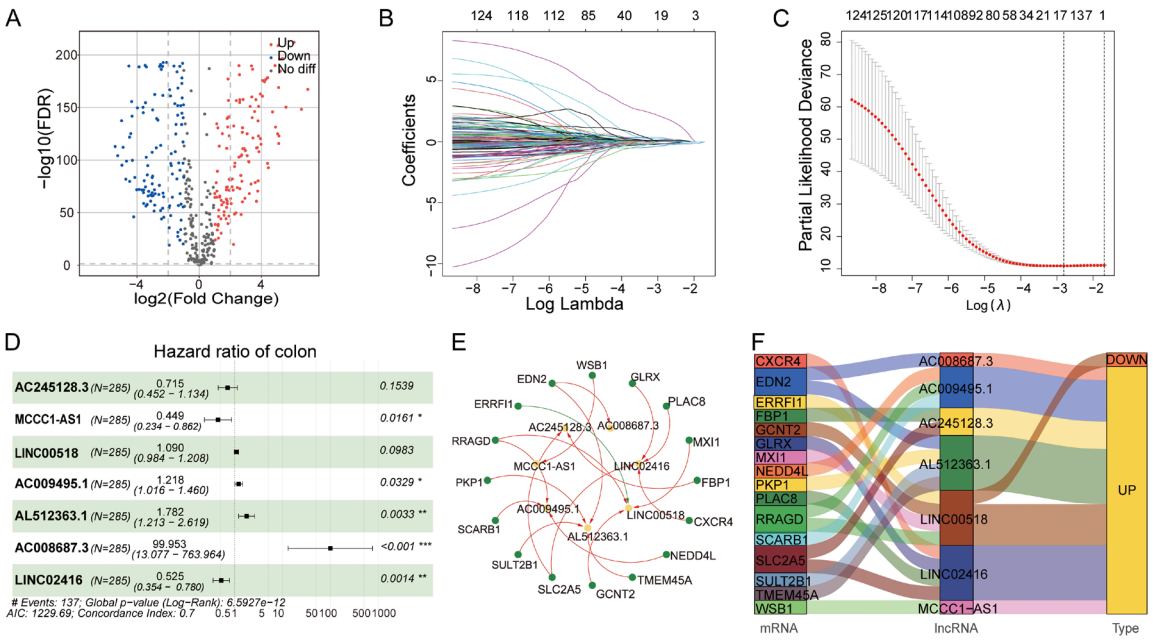

Figure 2. Hypoxia-related lncRNAs were identified by screening via LASSO and multivariate Cox regression analyses. A. Volcano map of differentially expressed hypoxia-related lncRNAs based on the TCGA and GTEx databases. B. LASSO coefficient profiles of the 126 candidate lncRNAs. C. Tuning parameter λ in the LASSO model. D. Seven hypoxia-related lncRNAs were ultimately identified by multivariate Cox regression analyses. E. The interaction network of hypoxia-related genes and the seven hypoxia-related lncRNAs was visualized using Cytoscape. F. Sankey diagrams of hypoxia-related genes and seven hypoxia-related lncRNAs.

AC008687.3, LINC00518, and AC009495.1 in the high-risk group were greater than those in the low-risk group, and the AC245128.3, LINC02416, and MCCCA-AS1 expression levels were lower in the high-risk group than in the low-risk group.

Relationships between the risk score based on the prognostic signature and clinical features

To further explore the correlation between hypoxia-related lncRNAs and the clinical characteristics of melanoma patients in the total TCGA dataset, patients were divided into two groups according to age (<65/≥65), sex (female/male), and stage (I+II/III+IV). The stratified analysis results showed that the signature performed well in distinguishing subgroups (**Figure 4A-F**). Moreover, in the subgroup analysis according to clinical features, OS was significantly longer in the low-risk group than in the high-risk group. The detailed distribution of the clinical characteristics of the two risk groups is shown in the heatmap (**Figure 4G**). The risk classification of melanoma samples in the TCGA cohort was also visualized clearly by principal component analysis (**Figure 4H**). In addition, the Kaplan-Meier curves of each of the seven hypoxia-related lncRNAs are shown in Supplementary Figure 2. The median expression value of each lncRNA was used as a cutoff value for classifying patients into high- and low-risk groups. AL512363.1 and AC008687.3 expression was not detected in some samples, so positive expression of these factors was used to differentiate between high- and low-risk patients.

Construction of the nomogram and evaluation of its performance

To verify whether the risk score can be used as an independent prognostic biomarker, the risk score and clinicopathological factors, such as age, sex, stage, pathological T stage, pathological M stage, and pathological N stage, were included as covariates. Univariate and multivariate Cox regression analyses were applied for training, testing, and entire cohort analyses, respectively (**Figure 5A-F**). The results indicated that the risk score served as an independent prognostic factor. Finally, a nomogram was established with age, pathological T stage, pathological N stage, and the risk score as covariates (**Figure 5G**). The AUC values for 3-, 5-, and 10-year OS predictions were greater

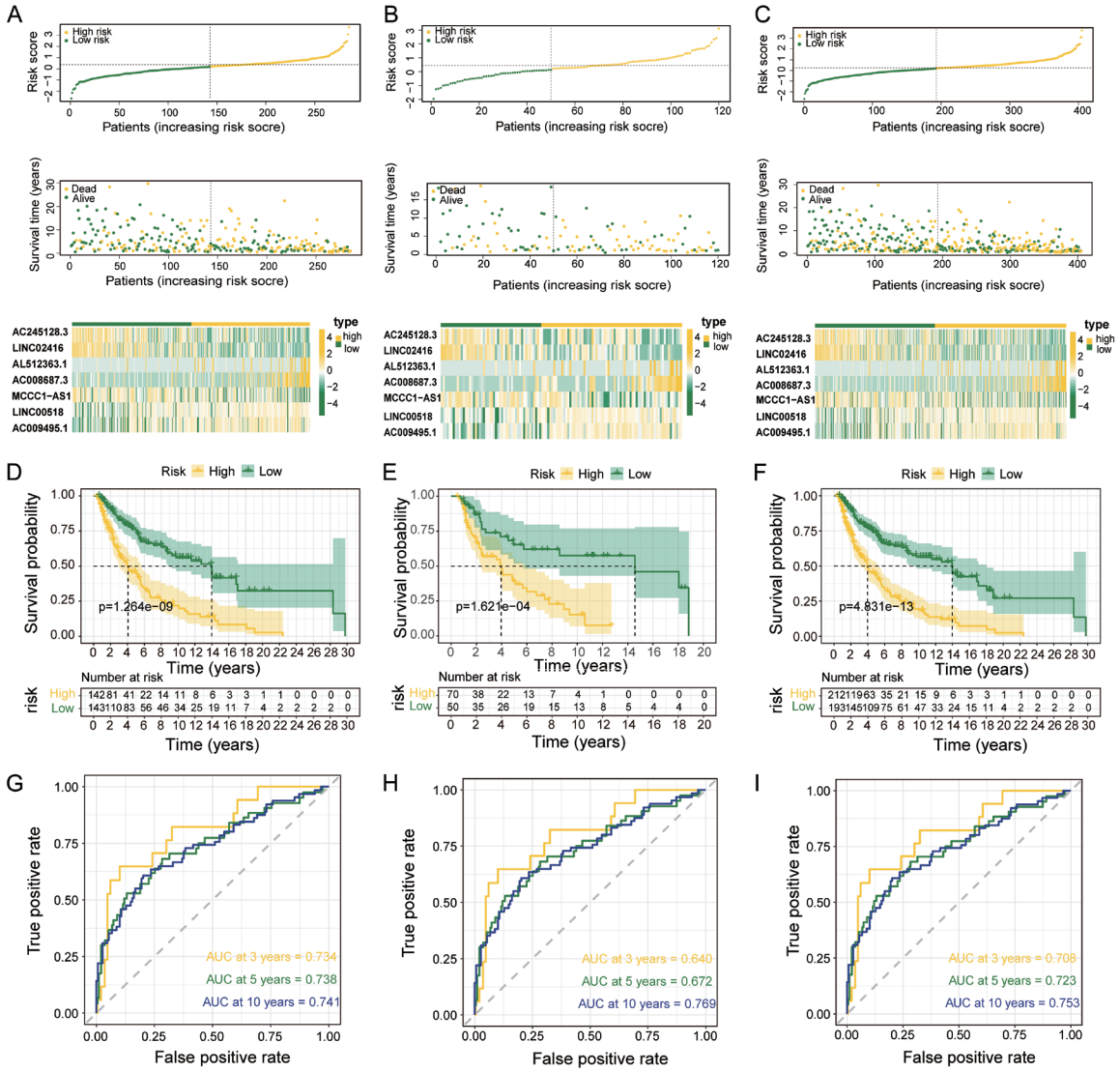

Figure 3. The prognostic value of the risk model consisting of seven hypoxia-related lncRNAs was assessed in the training cohort, testing cohort, and entire cohort. Distribution of the risk score, survival time and survival status and heatmaps of the expression of the seven hypoxia-related signature lncRNAs in the training cohort (A), testing cohort (B), and entire cohort (C). Kaplan-Meier OS curves for melanoma patients in the two risk subgroups in the training cohort (D), testing cohort (E), and entire cohort (F). The ROC curve was used to verify the prognostic value of the hypoxia-related lncRNAs at 3-, 5- and 10-year in the training cohort (G), testing cohort (H), and entire cohort (I).

than 0.79 (**Figure 5H**). In addition, according to result of the decision curve analysis for 3-, 5-year survival, if the threshold probability of patients is between 10 and 75%, the nomogram based on the risk score performed better in net benefit than tumor stage and TNM stage respectively (**Figure 5I**). The calibration curves also showed that the nomogram was able to predict 3-, 5-, and 10-year OS accurately (**Figure 5J**). These results indicate that the nomogram has high accuracy for predicting 3-, 5- and 10-year OS in melanoma patients.

Enrichment analysis of hypoxia-related lncRNAs in the prognostic signature

The above results indicated that melanoma patients in different groups have differences in OS. GO enrichment (**Figure 6A**, **6B**) and KEGG enrichment (**Figure 6C**, **6D**) analyses of the differentially expressed genes (DEGs) between two risk subgroups in the training cohort were performed. The circular diagrams depict the DEGs between the two risk subgroups and the GO terms and KEGG pathways in which they

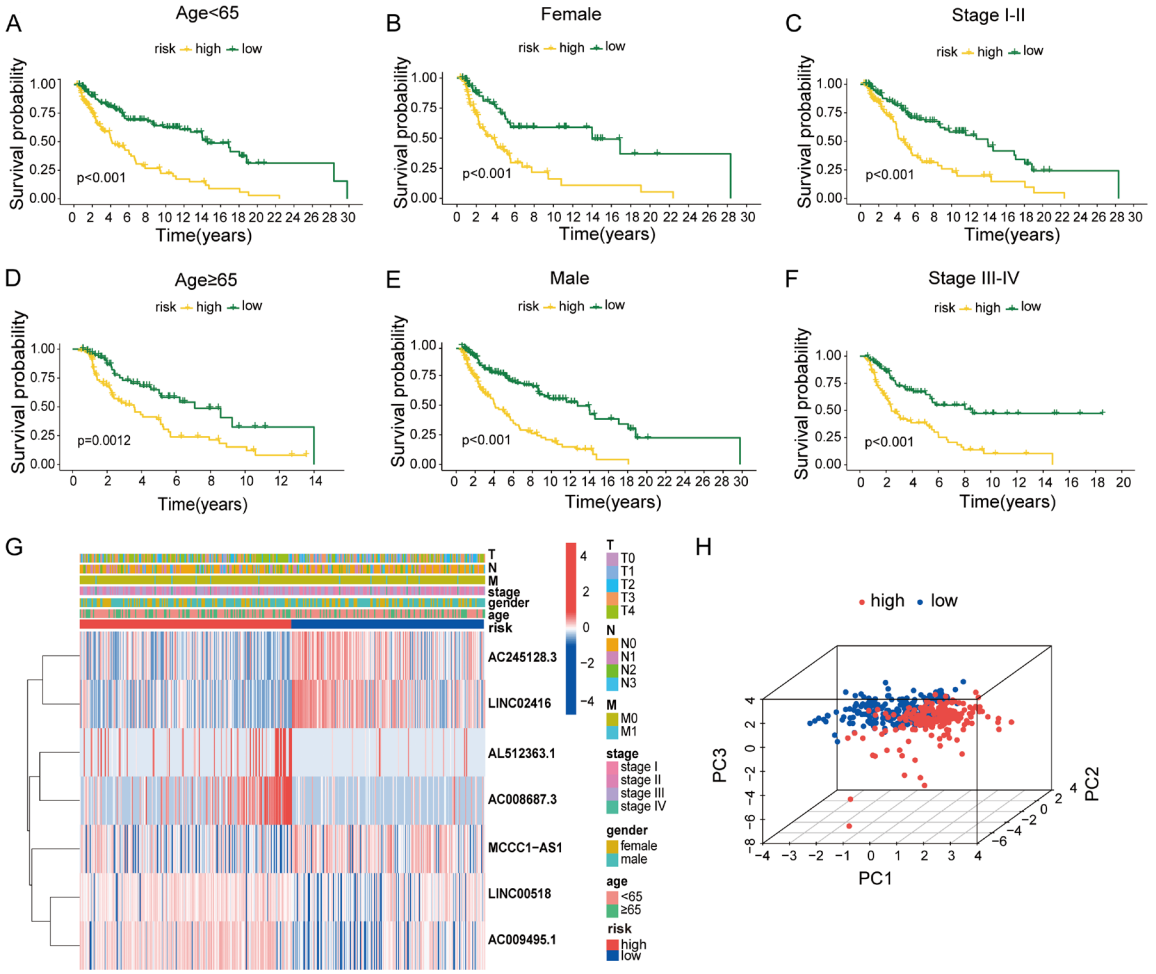

Figure 4. The clinicopathological characteristics of melanoma patients in different risk subgroups. A-F. The Kaplan-Meier curves of OS for patients in the two subgroups in the entire cohort stratified by age, sex, and stage. G. The heatmap showed the expression of seven hypoxia-related lncRNAs in patients with different clinicopathological features. H. The distribution of melanoma samples in different risk groups, as determined by principal component analysis (PCA), was visualized via a 3D scatterplot.

were significantly enriched (Supplementary Figure 3). GSEA was used to identify potential enriched pathways in the high-risk and low-risk groups. A NOM *p*-value <0.05, |NES|>1.0, and FDR<0.25 were used as the cutoff values. The enrichment results revealed that genes upregulated in the high-risk group were enriched in the following pathways: estrogen response early and late, glycolysis, KRAS signaling, MYC targets v2, and oxidative phosphorylation (**Figure 6E**). Genes upregulated in the low-risk group were enriched in immune response-related pathways, such as allograft rejection, IL6-JAK-STAT3 signaling, inflammatory response, interferon alpha and gamma response, and TNFA signaling via NFKB (**Figure 6F**).

Correlation analysis of the prognostic signature and tumor immune microenvironment

Correlation analysis of immune cells infiltration levels and the risk score revealed that the risk score was positively correlated with the levels of M0 and M2 macrophages and negatively correlated with the levels of CD8 T cells and mDCs (**Figure 7A**). We subsequently used the CIBERSORT algorithm to assess immune infiltration in melanoma tissues in the high-risk and low-risk groups. The results revealed that M0 and M2 macrophages and resting mast cells were more abundant in the high-risk group. The low-risk group was more enriched in plasma cells, CD8 T cells, activated memory

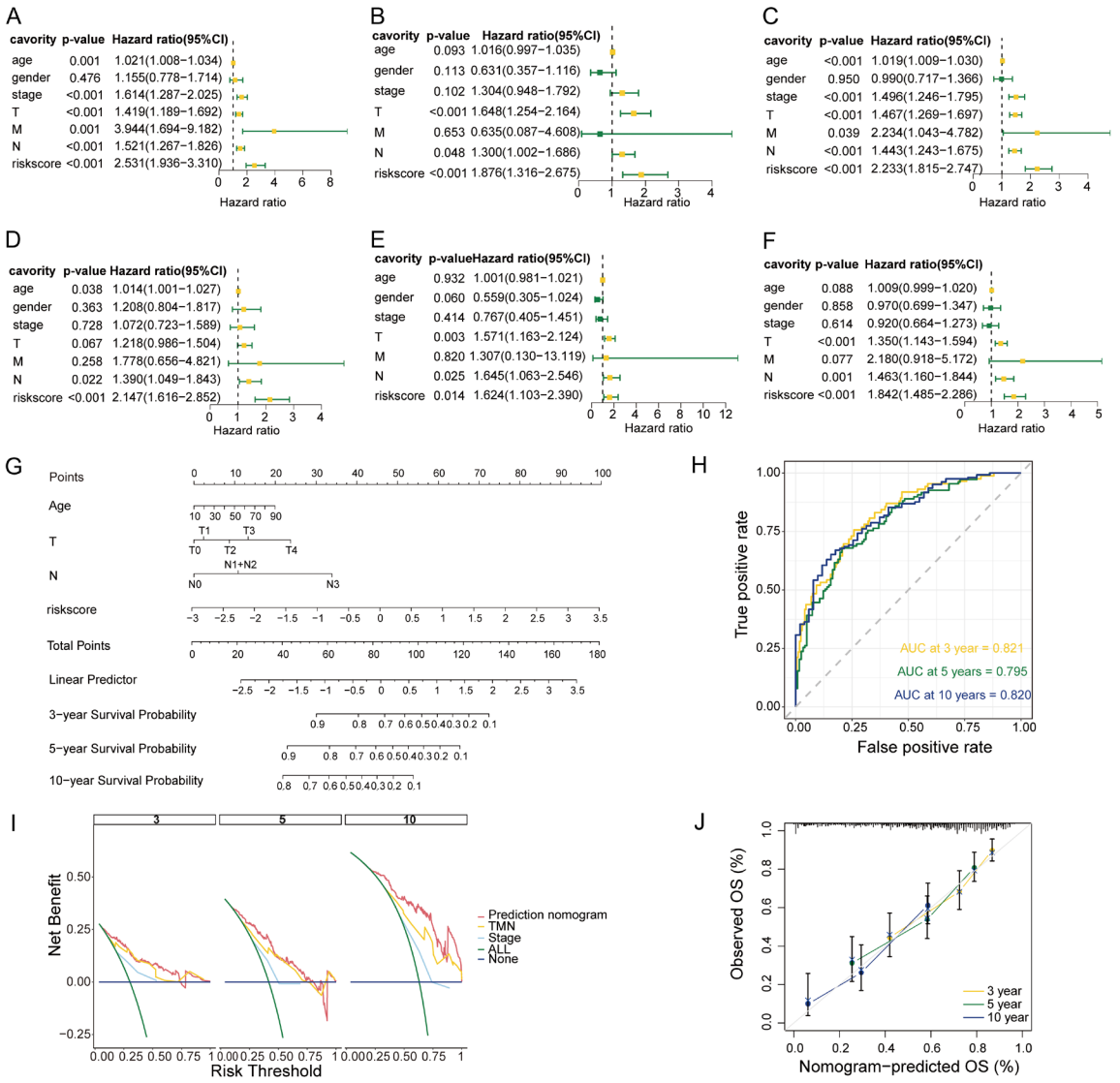

Figure 5. Nomogram construction and analysis of the prognostic value of seven hypoxia-related lncRNAs. Univariate Cox regression analysis of OS in the training cohort (A), testing cohort (B), and entire cohort (C). Multivariate Cox regression analyses of the training cohort (D), testing cohort (E), and entire cohort (F). (G) The nomogram for predicting the 3-, 5- and 10-year OS of patients with melanoma. (H) ROC curve analysis of the ability of the nomogram to predict 3-, 5- and 10-year OS. (I) Decision curve analysis of the nomogram for predicting 3-, 5- and 10-year OS in patients stratified by the risk score, TNM stage, and tumor stage. (J) Calibration curves of the nomogram.

CD4 T cells, regulatory T cells (Tregs), activated NK cells, monocytes, and M1 Macrophages (**Figure 7B**). In addition, according to the ssGSEA results, in addition to CD56dim natural killer (NK) cells, 27 other types of immune cells were significantly differentially enriched between the two risk subgroups (**Figure 7C**, Supplementary Figure 4). We applied the ESTIMATE algorithm to assess immune scores in the two groups. The Stromal score, immune score, and ESTIMATE score were significantly different between the low-risk group and the high-risk group (**Figure 7D**). Moreover, the tumor purity was greater in the high-risk group than in the low-risk group (**Figure 7E**). These results indicated that a decrease in the proportion of infiltrating immune cells was correlated with tumor growth and progression.

Association of immune checkpoint expression, the immunotherapy response, and the IPS with the risk score based on the prognostic signature

Given that immunotherapy is currently the primary treatment for melanoma, we analyzed the

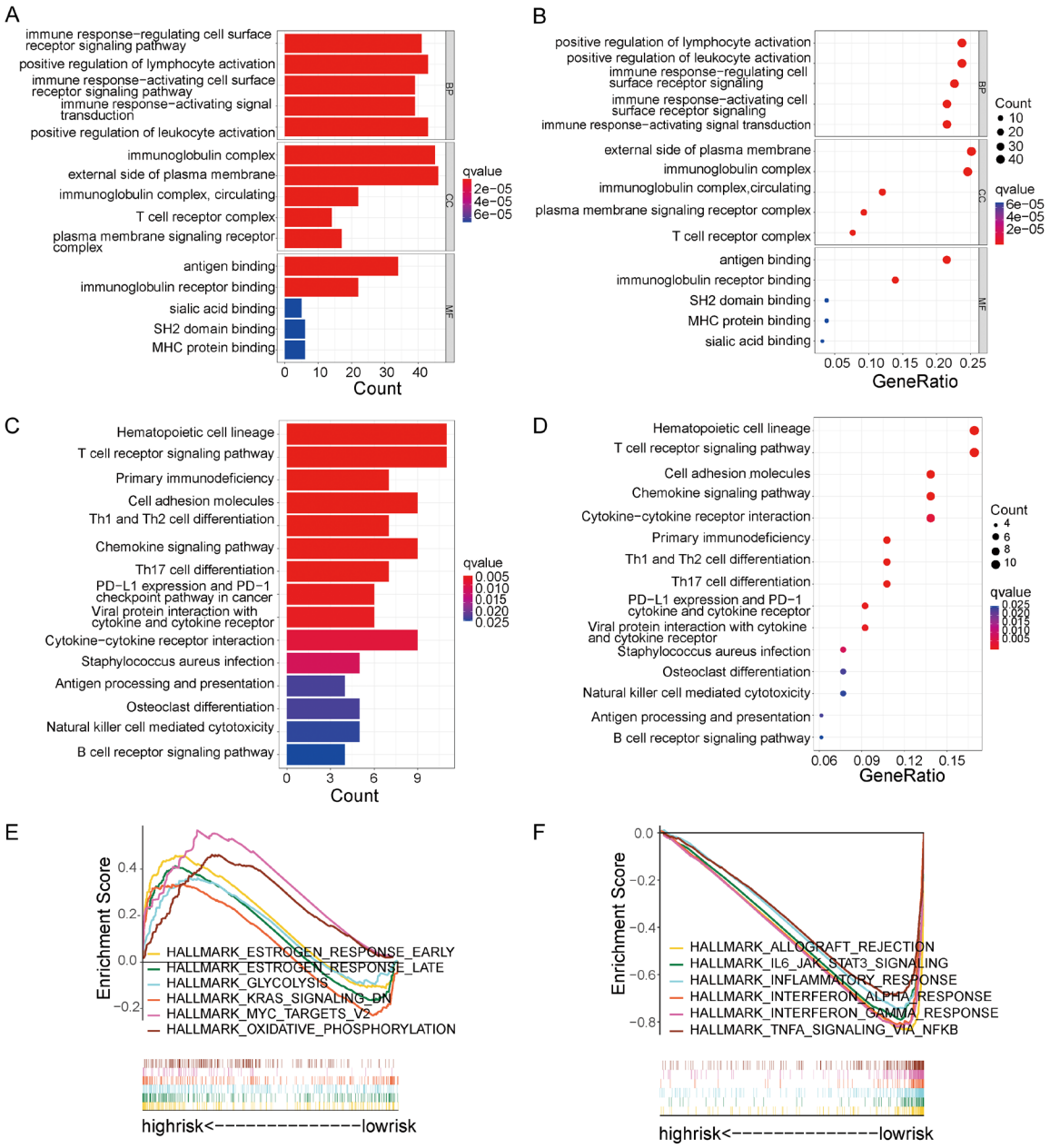

Figure 6. Functional and significant pathways enrichment analysis. Enrichment analyses of differentially expressed genes between two subgroups by GO (A, B) and KEGG (C, D). Gene Set Enrichment Analysis results of the HALLMARK pathways in the high-risk group (E) and low-risk group (F).

expression of immune checkpoint genes in the two risk groups and the correlations between the risk score and the expression levels of five immune checkpoint genes (CD274, PDCD1, CTLA4, LAG3, and HAVCR2). The results showed that the expression of most immune checkpoint genes was significantly greater in the low-risk group (**Figure 8A**, **8B**). In addition, the risk score was negatively related to the expression levels of all five immune checkpoint molecules (**Figure 8C-G**). The IPS, an excellent predictor of prognosis, was correlated with the response to anti-CTLA-4 and anti-PD-1 antibodies [27]. A high IPS was correlated with greater immune reactivity. The low-risk group had better immunotherapeutic efficacy, especially for patients receiving anti-PD-1 therapy (**Figure 8H**). The new ImmuCellAI algorithm could predict immunotherapy response with high accuracy [28]. The response to immunotherapy in

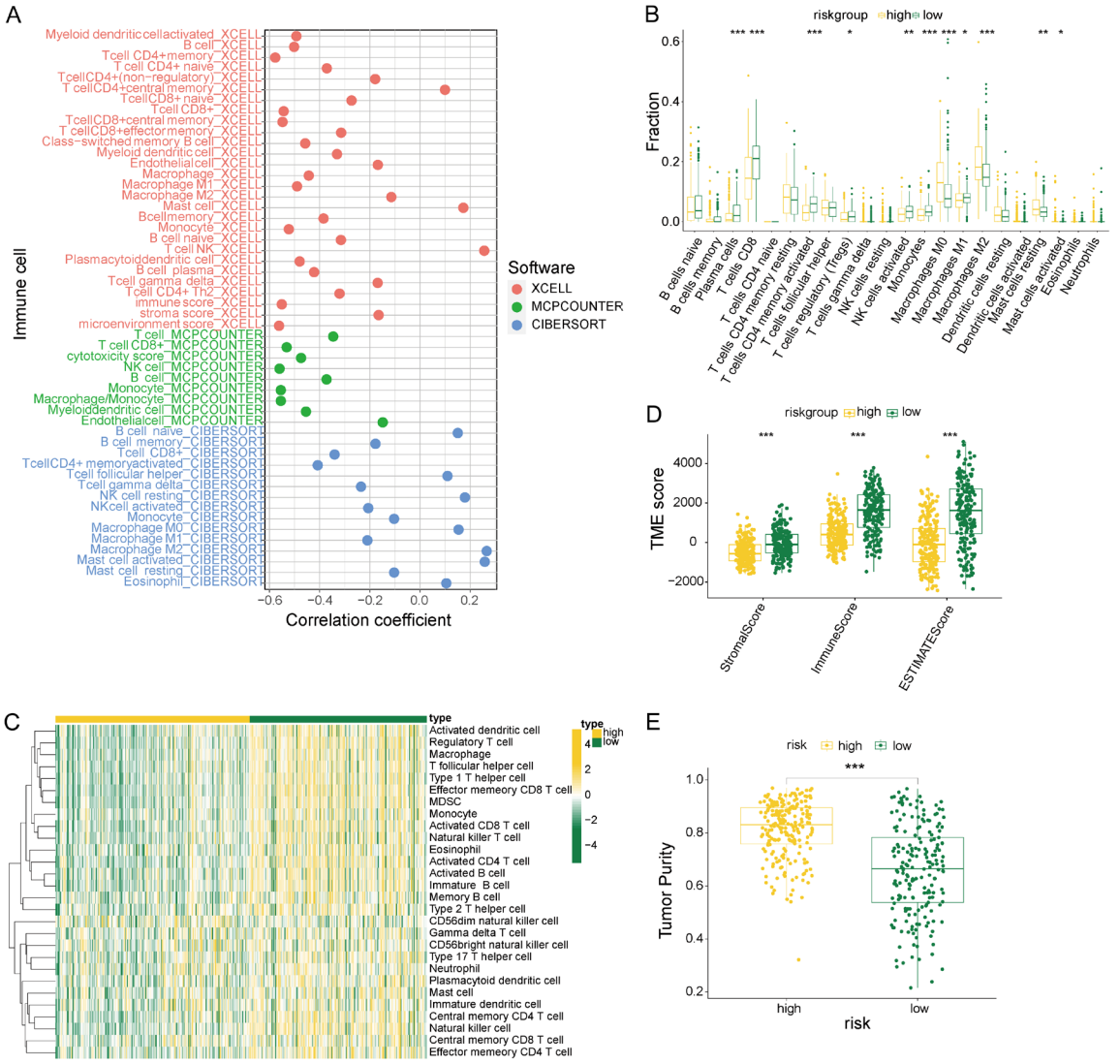

Figure 7. Seven hypoxia-related lncRNAs associated with the immune microenvironment. A. Analyses results of correlation coefficients between immune cell proportions and risk score in various software. B. Comparison of immune cell proportions by CIBERSORT. C. Correlation between the risk score and 28 immune cell types in the ssGSEA approach. D. Stromal score, Immune score, and ESTIMATE score between two risk subgroups. E. Tumor purity between two risk subgroups.

the two risk subgroups is shown in **Figure 8I**. As expected, the immunotherapy response rate was higher in the low-risk group.

Association of the mutation landscape and TMB with the risk score based on the prognostic signature

To further evaluate the differences in mutation profiles between the high and low-risk groups, the tumor mutation burden, a biomarker that can help predict a patient's response to immunotherapy, was compared between the two risk groups. Regrettably, we did not observe a significant difference between groups (**Figure 9A**). However, according to the survival curves of the high- and low-TMB groups, the survival rate was higher in the high-TMB subgroup (**Figure 9B**). Furthermore, when TMB and risk score were both considered, the prognosis of patients in the high-TMB/low-risk group was significantly greater than that of patients in the other three groups (**Figure 9C**). Next, we identified the top 20 genes in terms of alteration frequency in the risk subgroups (**Figure 9D-G**). Missense and nonsense mutations were the two most com-

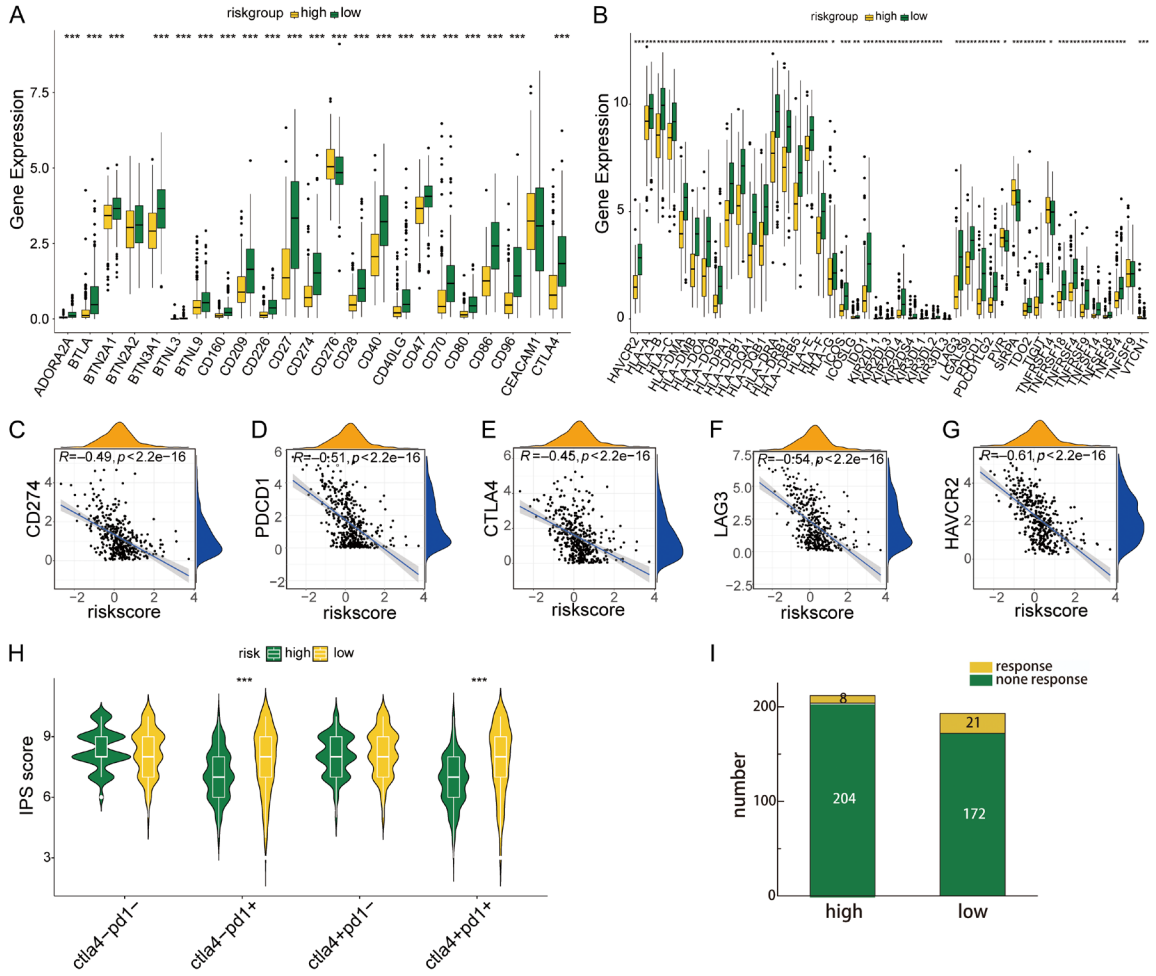

Figure 8. Analysis of the benefits of immunotherapy in two risk subgroups. The expression of immune checkpoint genes in different risk groups (A, B). The correlation of common immune checkpoints and risk score in the entire cohort. (C) CD274. (D) PDCD1. (E) CTLA4. (F) LAG3. (G) HAVCR2. (H) Results of IPS scores for predicting patient response to immune checkpoint inhibitors. (I) The counts of responder and non-responder to immunotherapy in two risk subgroups.

mon mutation types. Notably, TTN, MUC16, DNAH5, BRAF, and PCLO were among the five genes most frequently mutated in both the high-risk group and the low-risk group.

Prediction of chemotherapeutic drug sensitivity

To evaluate the value of the risk score in predicting the treatment response of melanoma patients, we analyzed the relationship between the risk score and the efficacy of chemotherapeutic drugs. Our study showed that the risk score was significantly associated with the IC50 of chemotherapeutic agents. The low-risk group was more sensitive to treatment with Axitinib, Leflunomide, Navitoclax, Niraparib, Oxaliplatin, Palbociclib, Ribociclib, Ruxolitinib, Temozolomide, and Venetoclax than the high-risk group (**Figure 10A-J**). However, the high-risk group was more sensitive to Selumetinib and Lapatinib than the low-risk group (**Figure 10K**, **10L**).

Discussion

Melanoma has attracted the attention of many medical researchers due to its high metastasis rate and poor prognosis. The immuno-oncology agents and targeted therapies has facilitated an increase in the survival rate of melanoma patients [29]. Nevertheless, side effects and immune resistance can occur [6, 30]. Hypoxia is a common cancer microenvironment feature

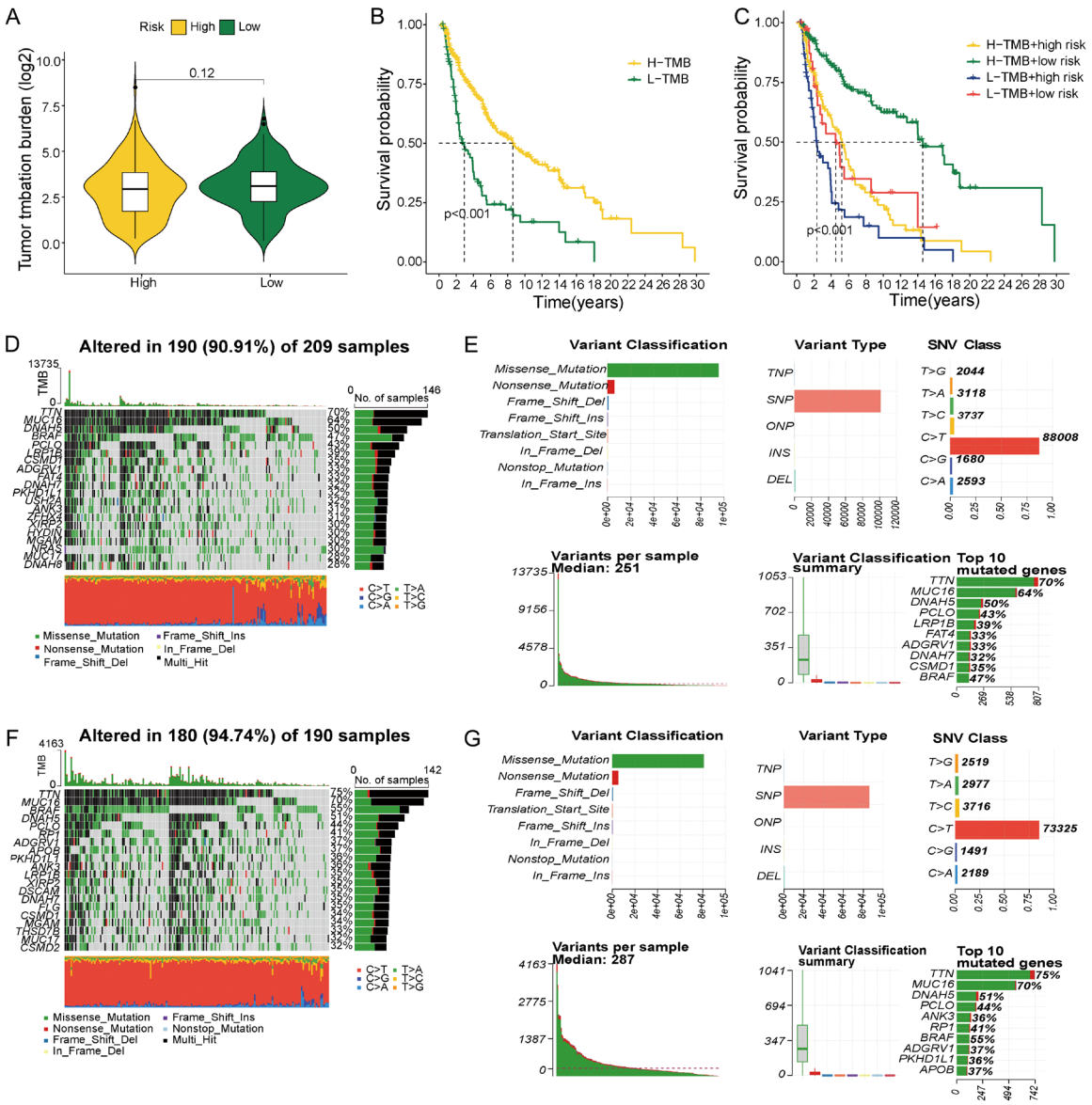

Figure 9. Mutation landscape and TMB in risk subgroups. (A) TMB difference in the high- and low-risk patients. (B) Kaplan-Meier curves between high and low TMB groups. (C) Kaplan-Meier curves with different risk and TMB. Mutation landscape in the high-risk group (D, E) and low-risk group (F, G).

and a potential limiting factor in cancer treatment. According to the latest article, reducing the degree of hypoxia through physical exercise can attenuate cancer stemness and suppress hepatocellular carcinoma progression [31]. However, there are few prognostic signatures related to hypoxia-related lncRNAs in melanoma. In-depth screening of lncRNAs that can act as reliable predictive biomarkers is a key strategy for improving the prognosis and treatment of melanoma.

In the present study, AC245128.3, LINC02416, AL512363.1, AC008687.3, MCCC1-AS1, LINC00518, and AC009495.1 were identified as prognostic lncRNAs and incorporated into a model for predicting in melanoma prognosis. Multiple analyses indicated that the risk model has excellent accuracy and stability. The ROC curve and univariate and multivariate Cox regression results showed that the risk model has excellent accuracy and stability and that the risk score could be used as an independent risk factor for estimating the prognosis of patients with melanoma. Among the seven hypoxia-related lncRNAs, AC245128.3, LINC02416, and MCCC1-AS1 were upregulated and were found to be beneficial factors in mela-

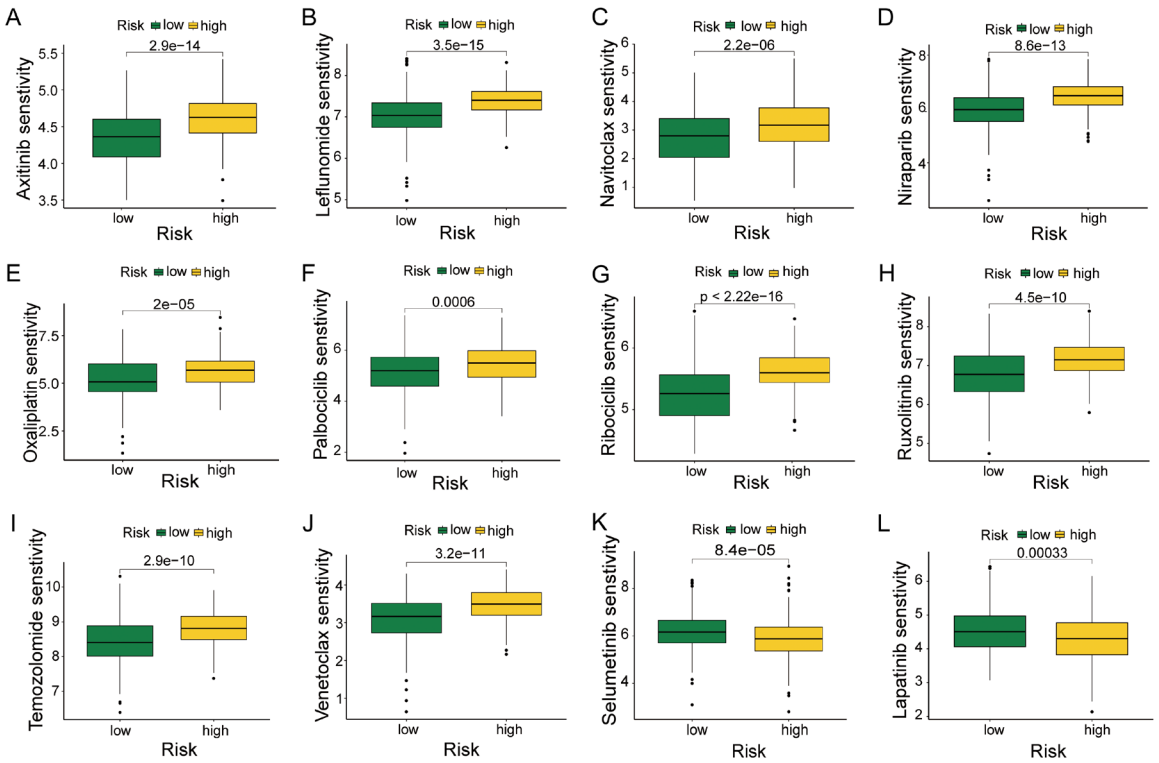

Figure 10. Prediction of chemotherapeutic drug sensitivity in different risk subgroups. A. Axitinib. B. Leflunomide. C. Navitoclax. D. Niraparib. E. Oxaliplatin. F. Palbociclib. G. Ribociclib. H. Ruxolitinib. I. Temozolomide. J. Venetoclax. K. Selumetinib. L. Lapatinib.

noma patients. Upregulation of LINC00518, AC008687.3, AC009495.1, and AL512363.1 expression was correlated with a high risk score. Notably, LINC00518, the most highly expressed lncRNA among the seven identified lncRNAs, has been implicated in a variety of cancers, including lung adenocarcinoma [32], colorectal cancer [33], and head and neck squamous cell carcinoma [34]. In uveal melanoma, LINC00518 acts as an oncogene, and transient silencing of LINC00518 in vitro affects cell proliferation and migration [35]. LINC00518 promotes malignant behaviors by influencing EIF4A3-mediated MITF mRNA stability [36], and the miR-204-5p/AP1S2 axis promotes the metastasis of malignant melanoma [37]. Knockdown of LINC00518 in cutaneous malignant melanoma cells significantly inhibited cell invasion, migration, proliferation, and clonogenicity [38]. Moreover, researchers have used LINC00518 as a potential gene for evaluating suspicious pigmented lesions (specifically, for distinguishing between melanoma and nonmelanoma samples) [39] and for 3-GEP pigmented lesion assays to guide the assessment and treatment of pigmented dermatoses [40]. Interestingly, in our study, GSEA revealed enrichment of the glycolytic pathway in the high-risk group. It has been reported that the overexpression of glycolysis-related molecules may decrease the cytotoxicity of T cells against melanoma cells [41]. Other enriched pathways in the high-risk group were the estrogen response and oxidative phosphorylation pathways. Previous studies have indicated that estrogen stimulates melanoma growth by disrupting macrophage polarization, which confers an immunosuppressive state and promotes CD8+ T cell resistance to immune checkpoint blockade [42]. Promotion of intracellular oxidative phosphorylation and glycolysis is associated with immune checkpoint inhibitor resistance [43].

Coincidentally, AC008687.3 was shown to be a differentially expressed glycolysis-related lncRNA in pancreatic ductal adenocarcinoma [44]. We speculate that AC008687.3 may impair the killing power of T cells through the glycolytic pathway in melanoma patients. In

addition, AC245128.3 may influence cell pyroptosis and necroptosis in cancer. It has been reported that AC245128.3 influences the prognosis of cutaneous melanoma [45] and acts as a necroptosis-related prognostic lncRNA signature in ovarian cancer [46]. Furthermore, AL512363.1 was identified by screening as a differentially expressed lncRNAs in metastatic melanoma [47]. AC009495.1 was identified as a prognostic lncRNA related to epithelial-mesenchymal transition in the melanoma microenvironment [48], but the underlying mechanisms of AL512363.1 and AC009495.1 are unclear. LINC02416 and MCCC1-AS1 were first discovered in melanoma. It has been reported that MCCC1-AS1 may be related to the prognosis of endometrial carcinoma of the uterine corpus [49]. LINC02416 is highly expressed in hepatocellular carcinoma [50]. The underlying mechanisms by which these lncRNAs exert their effects deserve further study.

Immunotherapy represents a significant breakthrough in the treatment of metastatic melanoma. The emergence of tumor immunotherapy has transformed healthcare for cancer patients [51]. In recent years, the main immunotherapy strategies have shifted from cytokine-based therapies to antibody-mediated blockade of CTLA-4 and PD-1 [52]. Among these, antibody-based immune checkpoint agents, anti-CTLA4 and anti-PD-1 antibodies can alter the course of advanced melanoma by targeting and modulating the dysfunctional immune system [53]. Our study explored the relationship between these prognostic biomarkers and the response to immunotherapy. First, we analyzed the enrichment of pathways between the two risk subgroups via GSEA. According to the GSEA results, inflammation, the immune response, and interferon were the main enriched factors in the low-risk group. According to previous articles, T cells, CD8+ T cells, tertiary lymphoid structures (TLS), and mDCs/pDCs are associated with a favorable prognosis; M2 macrophages and neutrophils are associated with an unfavorable prognosis; and Tregs, B cells and mast cells had varied effects on melanoma prognosis [54]. According to the present analysis, the risk scores were positively correlated with M2 macrophages and negatively correlated with CD8+ mDCs. In line with the immune response results, the expression of most immune checkpoint genes was also greater in the low-risk group. These results demonstrated that immune cell status differences between the high- and low-risk groups may cause differential survival outcomes. Additionally, we calculated the response rate and IPS for the two risk groups. The response rate was greater in the low-risk group than in the high-risk group, suggesting that our signature has potential predictive value for the response to immunotherapy. According to the IPS results, particularly for patients receiving anti-PD-1 therapy, ICIs might be more beneficial in patients in the low-risk group.

The TMB and inflammatory gene expression profile are related to the clinical response to immunotherapy for advanced melanoma [55]. In cutaneous melanoma, the TMB was positively correlated with prognosis [56]. Unfortunately, there was no significant difference in TMB between the high-risk and low-risk groups; however, the low-risk group had slightly greater TMB than did the high-risk group. When both factors were considered, the high-TMB/low-risk groups was found to have a much better prognosis than the other groups. Finally, we used the “oncoPredict” R package to assess drug sensitivity. Our results confirm the potential value of the signature in predicting the sensitivity to several chemotherapeutic agents: Patients in the low-risk group were more sensitive to the majority of chemotherapy drugs than patients in the high-risk group.

In summary, we identified seven hypoxia-related lncRNAs and established a prognostic risk model. Patient stratification based on the risk score effectively predicted prognosis. In addition, the signature of seven prognostic lncRNAs may predict the response to immunotherapy. Inevitably, our study has several limitations, such as the limited availability of drugs for assessing drug sensitivity and insufficient external data for verifying the results. Continued research on immune-related therapies may lead to a cure for melanoma.

Conclusions

Our study identified a signature of seven hypoxia-related lncRNAs with excellent prognostic value in melanoma; this signature can be applied to evaluate melanoma prognosis and the response to immunotherapy.

Acknowledgements

This research was funded by the Science and Technology Commission of Shanghai Municipality, grant number: 20Y21900900, the First Affiliated Hospital of Navy Medical University, grant number: 2020YXK027, and the National Natural Science Foundation of China, grant number: 81871253. The authors thank Zhehan Yu for the linguistic editing of the manuscript.

Disclosure of conflict of interest

None.

Address correspondence to: Yanlong Yang, School of Traditional Chinese Medicine, Naval Medical University, Shanghai 200433, China. E-mail: yangyanlong@smmu.edu.cn; Ling Tang, Department of Traditional Chinese Medicine, The First Affiliated Hospital of Naval Medical University, Shanghai 200433, China. E-mail: tanglingyu@126.com; Yizhi Yu, National Key Laboratory of Immunity & Inflammation, Naval Medical University, Shanghai 200433, China. E-mail: yuyz@immunol.org

References

[1] Arnold M, Singh D, Laversanne M, Vignat J, Vaccarella S, Meheus F, Cust AE, de Vries E, Whiteman DC and Bray F. Global burden of cutaneous melanoma in 2020 and projections to 2040. JAMA Dermatol 2022; 158: 495-503.

[2] Pawlikowska M, Jędrzejewski T, Slominski AT, Brożyna AA and Wrotek S. Pigmentation levels affect melanoma responses to coriolus versicolor extract and play a crucial role in melanoma-mononuclear cell crosstalk. Int J Mol Sci 2021; 22: 5735.

[3] Sung H, Ferlay J, Siegel RL, Laversanne M, Soerjomataram I, Jemal A and Bray F. Global cancer statistics 2020: GLOBOCAN estimates of incidence and mortality worldwide for 36 cancers in 185 countries. CA Cancer J Clin 2021; 71: 209-249.

[4] Li Z, Fang Y, Chen H, Zhang T, Yin X, Man J, Yang X and Lu M. Spatiotemporal trends of the global burden of melanoma in 204 countries and territories from 1990 to 2019: results from the 2019 global burden of disease study. Neoplasia 2022; 24: 12-21.

[5] Rozeman EA, Dekker TJA, Haanen JBAG and Blank CU. Advanced melanoma: current treatment options, biomarkers, and future perspectives. Am J Clin Dermatol 2018; 19: 303-317.

[6] Gide TN, Wilmott JS, Scolyer RA and Long GV. Primary and acquired resistance to immune checkpoint inhibitors in metastatic melanoma. Clin Cancer Res 2018; 24: 1260-1270.

[7] Lin C and Yang L. Long noncoding RNA in cancer: wiring signaling circuitry. Trends Cell Biol 2018; 28: 287-301.

[8] Montico B, Giurato G, Pecoraro G, Salvati A, Covre A, Colizzi F, Steffan A, Weisz A, Maio M, Sigalotti L and Fratta E. The pleiotropic roles of circular and long noncoding RNAs in cutaneous melanoma. Mol Oncol 2022; 16: 565-593.

[9] Xu J, Shi A, Long Z, Xu L, Liao G, Deng C, Yan M, Xie A, Luo T, Huang J, Xiao Y and Li X. Capturing functional long non-coding RNAs through integrating large-scale causal relations from gene perturbation experiments. EBioMedicine 2018; 35: 369-380.

[10] Wang X, Ren Z, Xu Y, Gao X, Huang H and Zhu F. KCNQ1OT1 sponges miR-34a to promote malignant progression of malignant melanoma via upregulation of the STAT3/PD-L1 axis. Environ Toxicol 2023; 38: 368-380.

[11] Hanniford D, Ulloa-Morales A, Karz A, Berzoti-Coelho MG, Moubarak RS, Sánchez-Sendra B, Kloetgen A, Davalos V, Imig J, Wu P, Vasudevaraja V, Argibay D, Lilja K, Tabaglio T, Monteagudo C, Guccione E, Tsirigos A, Osman I, Aifantis I and Hernando E. Epigenetic silencing of CDR1as drives IGF2BP3-mediated melanoma invasion and metastasis. Cancer Cell 2020; 37: 55-70, e15.

[12] Riefolo M, Porcellini E, Dika E, Broseghini E and Ferracin M. Interplay between small and long non-coding RNAs in cutaneous melanoma: a complex jigsaw puzzle with missing pieces. Mol Oncol 2019; 13: 74-98.

[13] Li Y, Gao Y, Niu X, Tang M, Li J, Song B and Guan X. LncRNA BASP1-AS1 interacts with YBX1 to regulate Notch transcription and drives the malignancy of melanoma. Cancer Sci 2021; 112: 4526-4542.

[14] Chen Y, Cao K, Li J, Wang A, Sun L, Tang J, Xiong W, Zhou X, Chen X, Zhou J and Liu Y. Overexpression of long non-coding RNA NORAD promotes invasion and migration in malignant melanoma via regulating the MIR-205-EGLN2 pathway. Cancer Med 2019; 8: 1744-1754.

[15] D'Aguanno S, Mallone F, Marenco M, Del Bufalo D and Moramarco A. Hypoxia-dependent drivers of melanoma progression. J Exp Clin Cancer Res 2021; 40: 159.

[16] Malekan M, Ebrahimzadeh MA and Sheida F. The role of hypoxia-inducible factor-1alpha and its signaling in melanoma. Biomed Pharmacother 2021; 141: 111873.

[17] You L, Wu W, Wang X, Fang L, Adam V, Nepovimova E, Wu Q and Kuca K. The role of hypoxia-inducible factor 1 in tumor immune evasion. Med Res Rev 2021; 41: 1622-1643.

[18] Ke G, Cheng N, Sun H, Meng X and Xu L. Explore the impact of hypoxia-related genes (HRGs) in cutaneous melanoma. BMC Med Genomics 2023; 16: 160.
[19] Wang G, Sun Y and Xu Q. The development and experimental validation of hypoxia-related long noncoding RNAs prognostic signature in predicting prognosis and immunotherapy of cutaneous melanoma. Aging (Albany NY) 2023; 15: 11918-11939.
[20] Newman AM, Liu CL, Green MR, Gentles AJ, Feng W, Xu Y, Hoang CD, Diehn M and Alizadeh AA. Robust enumeration of cell subsets from tissue expression profiles. Nat Methods 2015; 12: 453-457.
[21] Yoshihara K, Shahmoradgoli M, Martínez E, Vegesna R, Kim H, Torres-Garcia W, Treviño V, Shen H, Laird PW, Levine DA, Carter SL, Getz G, Stemke-Hale K, Mills GB and Verhaak RG. Inferring tumour purity and stromal and immune cell admixture from expression data. Nat Commun 2013; 4: 2612.
[22] Dummer R, Ascierto PA, Nathan P, Robert C and Schadendorf D. Rationale for immune checkpoint inhibitors plus targeted therapy in metastatic melanoma: a review. JAMA Oncol 2020; 6: 1957-1966.
[23] Hu FF, Liu CJ, Liu LL, Zhang Q and Guo AY. Expression profile of immune checkpoint genes and their roles in predicting immunotherapy response. Brief Bioinform 2021; 22: bbaa176.
[24] Kalaora S, Nagler A, Wargo JA and Samuels Y. Mechanisms of immune activation and regulation: lessons from melanoma. Nat Rev Cancer 2022; 22: 195-207.
[25] Maeser D, Gruener RF and Huang RS. oncoPredict: an R package for predicting *in vivo* or cancer patient drug response and biomarkers from cell line screening data. Brief Bioinform 2021; 22: bbab260.
[26] Bland JM and Altman DG. The logrank test. BMJ 2004; 328: 1073.
[27] Charoentong P, Finotello F, Angelova M, Mayer C, Efremova M, Rieder D, Hackl H and Trajanoski Z. Pan-cancer immunogenomic analyses reveal genotype-immunophenotype relationships and predictors of response to checkpoint blockade. Cell Rep 2017; 18: 248-262.
[28] Miao YR, Zhang Q, Lei Q, Luo M, Xie GY, Wang H and Guo AY. ImmuCellAI: a unique method for comprehensive T-cell subsets abundance prediction and its application in cancer immunotherapy. Adv Sci (Weinh) 2020; 7: 1902880.
[29] Michielin O, Atkins MB, Koon HB, Dummer R and Ascierto PA. Evolving impact of long-term survival results on metastatic melanoma treatment. J Immunother Cancer 2020; 8: e000948.
[30] Rizk EM, Seffens AM, Trager MH, Moore MR, Geskin LJ, Gartrell-Corrado RD, Wong W and Saenger YM. Biomarkers predictive of survival and response to immune checkpoint inhibitors in melanoma. Am J Clin Dermatol 2020; 21: 1-11.
[31] Xiao CL, Zhong ZP, Lü C, Guo BJ, Chen JJ, Zhao T, Yin ZF and Li B. Physical exercise suppresses hepatocellular carcinoma progression by alleviating hypoxia and attenuating cancer stemness through the Akt/GSK-3β/β-catenin pathway. J Integr Med 2023; 21: 184-193.
[32] Shen R, Cai X, Shen D, Zhang R, Zhang W, Zhang Y, Li Y, Wang A, Zeng Y, Zhu J, Liu Z and Huang JA. Long noncoding RNA LINC00518 contributes to proliferation and metastasis in lung adenocarcinoma via the miR-335-3p/CTHRC1 axis. Cell Death Discov 2022; 8: 98.
[33] Jafari N, Nasiran Najafabadi A, Hamzei B, Ataee N, Ghasemi Z, Sadeghian-Rizi T, Honardoost MA, Zamani A, Dolatabadi NF and Tabatabaeian H. ESRG, LINC00518 and PWRN1 are newly-identified deregulated lncRNAs in colorectal cancer. Exp Mol Pathol 2022; 124: 104732.
[34] Wang X, Shen J, Wang L, Deng L, Bo H, Luo Y and Cui Y. DNA hypomethylation and upregulated *LINC00518* acts as a promoter and biomarker in head and neck squamous cell carcinoma. Epigenomics 2023; 15: 293-306.
[35] Barbagallo C, Caltabiano R, Broggi G, Russo A, Puzzo L, Avitabile T, Longo A, Reibaldi M, Barbagallo D, Di Pietro C, Purrello M and Ragusa M. LncRNA LINC00518 acts as an oncogene in uveal melanoma by regulating an RNA-based network. Cancers (Basel) 2020; 12: 3867.
[36] Zhang P, Liu X, Pan G, Xu J, Shen B, Ding X and Lv W. LINC00518 promotes cell malignant behaviors via influencing EIF4A3-mediated mRNA stability of MITF in melanoma. Biomed Res Int 2022; 2022: 3546795.
[37] Luan W, Ding Y, Ma S, Ruan H, Wang J and Lu F. Long noncoding RNA LINC00518 acts as a competing endogenous RNA to promote the metastasis of malignant melanoma via miR-204-5p/AP1S2 axis. Cell Death Dis 2019; 10: 855.
[38] Liu Y, He D, Xiao M, Zhu Y, Zhou J and Cao K. Long noncoding RNA LINC00518 induces radioresistance by regulating glycolysis through an miR-33a-3p/HIF-1α negative feedback loop in melanoma. Cell Death Dis 2021; 12: 245.
[39] Gerami P, Yao Z, Polsky D, Jansen B, Busam K, Ho J, Martini M and Ferris LK. Development and validation of a noninvasive 2-gene molecular assay for cutaneous melanoma. J Am Acad Dermatol 2017; 76: 114-120, e112.
[40] Ludzik J, Becker AL, Latour E, Lee C and Witkowski A. Dermoscopic features associated

with 3-GEP PLA: LINC00518, PRAME, and TERT expression in suspicious pigmented lesions. Skin Res Technol 2023; 29: e13323.
[41] Cascone T, McKenzie JA, Mbofung RM, Punt S, Wang Z, Xu C, Williams LJ, Wang Z, Bristow CA, Carugo A, Peoples MD, Li L, Karpinets T, Huang L, Malu S, Creasy C, Leahey SE, Chen J, Chen Y, Pelicano H, Bernatchez C, Gopal YNV, Heffernan TP, Hu J, Wang J, Amaria RN, Garraway LA, Huang P, Yang P, Wistuba II, Woodman SE, Roszik J, Davis RE, Davies MA, Heymach JV, Hwu P and Peng W. Increased tumor glycolysis characterizes immune resistance to adoptive T cell therapy. Cell Metab 2018; 27: 977-987, e974.
[42] Chakraborty B, Byemerwa J, Shepherd J, Haines CN, Baldi R, Gong W, Liu W, Mukherjee D, Artham S, Lim F, Bae Y, Brueckner O, Tavares K, Wardell SE, Hanks BA, Perou CM, Chang CY and McDonnell DP. Inhibition of estrogen signaling in myeloid cells increases tumor immunity in melanoma. J Clin Invest 2021; 131: e151347.
[43] Li C, Phoon YP, Karlinsey K, Tian YF, Thapaliya S, Thongkum A, Qu L, Matz AJ, Cameron M, Cameron C, Menoret A, Funchain P, Song JM, Diaz-Montero CM, Tamilselvan B, Golden JB, Cartwright M, Rodriguez A, Bonin C, Vella A, Zhou B and Gastman BR. A high OXPHOS CD8 T cell subset is predictive of immunotherapy resistance in melanoma patients. J Exp Med 2022; 219: e20202084.
[44] Zhu LL, Wu Z, Li RK, Xing X, Jiang YS, Li J, Wang YH, Hu LP, Wang X, Qin WT, Sun YW, Zhang ZG, Yang Q and Jiang SH. Deciphering the genomic and lncRNA landscapes of aerobic glycolysis identifies potential therapeutic targets in pancreatic cancer. Int J Biol Sci 2021; 17: 107-118.
[45] Xie J, Li H, Chen L, Cao Y, Hu Y, Zhu Z, Wang M and Shi J. A novel pyroptosis-related lncRNA signature for predicting the prognosis of skin cutaneous melanoma. Int J Gen Med 2021; 14: 6517-6527.
[46] Zhu L, He J, Yang X, Zheng J, Liu W and Chen H. Derivation and validation of a necroptosis-related lncRNA signature in patients with ovarian cancer. J Oncol 2022; 2022: 6228846.
[47] Sun L, Guan Z, Wei S, Tan R, Li P and Yan L. Identification of long non-coding and messenger RNAs differentially expressed between primary and metastatic melanoma. Front Genet 2019; 10: 292.
[48] Xiao B, Liu L, Chen Z, Li A, Wang P, Xiang C, Zeng Y, Li H and Xiao T. Identification of epithelial-mesenchymal transition-related prognostic lncRNAs biomarkers associated with melanoma microenvironment. Front Cell Dev Biol 2021; 9: 679133.
[49] Wang P, Zeng Z, Shen X, Tian X and Ye Q. Identification of a multi-RNA-type-based signature for recurrence-free survival prediction in patients with uterine corpus endometrial carcinoma. DNA Cell Biol 2020; 39: 615-630.
[50] Lin H, Xie Y, Kong Y, Yang L and Li M. Identification of two molecular subtypes of hepatocellular carcinoma based on dysregulated immune LncRNAs. Front Mol Biosci 2021; 8: 625858.
[51] Zhang N and Xiao XH. Integrative medicine in the era of cancer immunotherapy: challenges and opportunities. J Integr Med 2021; 19: 291-294.
[52] Luke JJ, Flaherty KT, Ribas A and Long GV. Targeted agents and immunotherapies: optimizing outcomes in melanoma. Nat Rev Clin Oncol 2017; 14: 463-482.
[53] Carlino MS, Larkin J and Long GV. Immune checkpoint inhibitors in melanoma. Lancet 2021; 398: 1002-1014.
[54] Galon J and Bruni D. Tumor immunology and tumor evolution: intertwined histories. Immunity 2020; 52: 55-81.
[55] Hodi FS, Wolchok JD, Schadendorf D, Larkin J, Long GV, Qian X, Saci A, Young TC, Srinivasan S, Chang H, Tang H, Wind-Rotolo M, Rizzo JI, Jackson DG and Ascierto PA. TMB and inflammatory gene expression associated with clinical outcomes following immunotherapy in advanced melanoma. Cancer Immunol Res 2021; 9: 1202-1213.
[56] Kang K, Xie F, Mao J, Bai Y and Wang X. Significance of tumor mutation burden in immune infiltration and prognosis in cutaneous melanoma. Front Oncol 2020; 10: 573141.

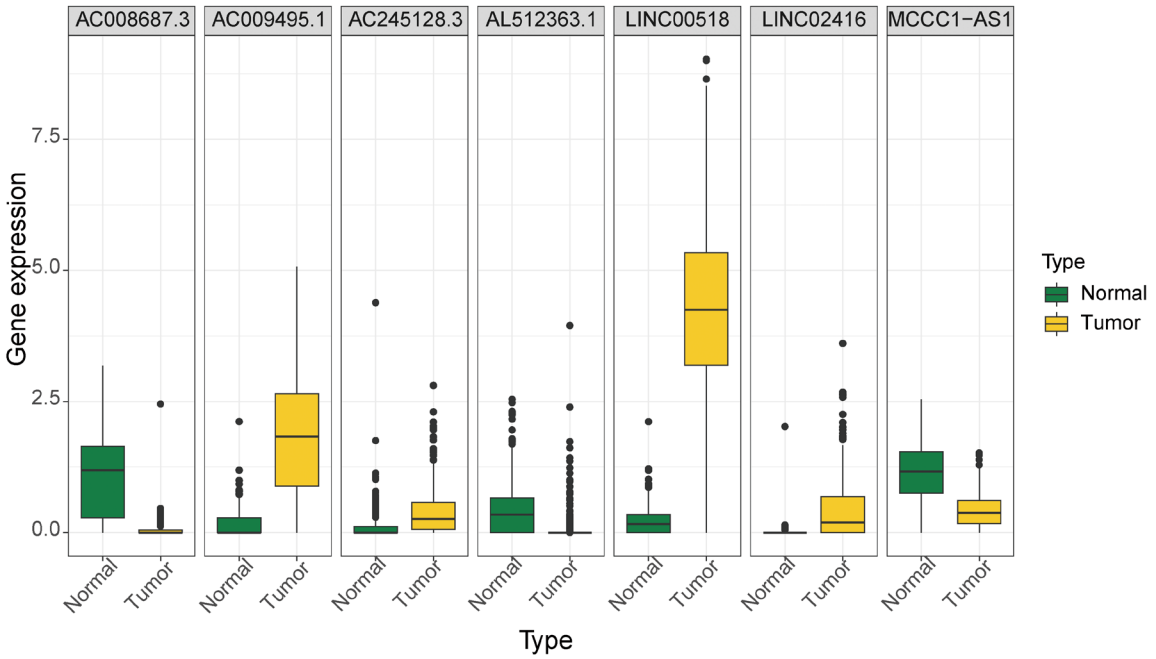

Supplementary Figure 1. Expression of seven hypoxia-related lncRNAs in the normal and tumor samples in TCGA and GTEx databases.

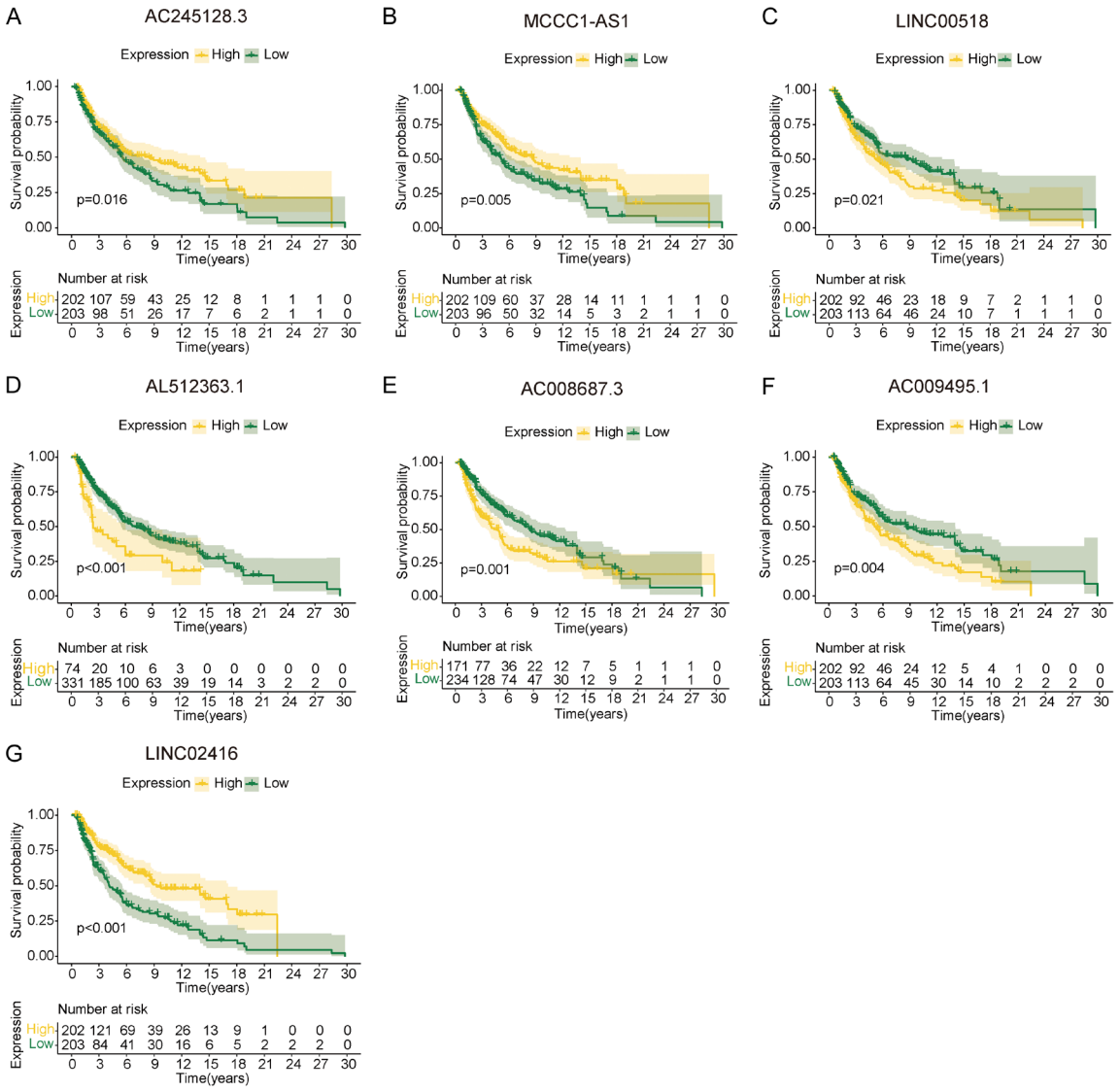

Supplementary Figure 2. Survival curves for each of seven hypoxia-associated lncRNA. A. AC245128.3. B. MCCC1-AS1. C. LINC00518. D. AL512363.1. E. AC008687.3. F. AC009495.1. G. LINC02416.

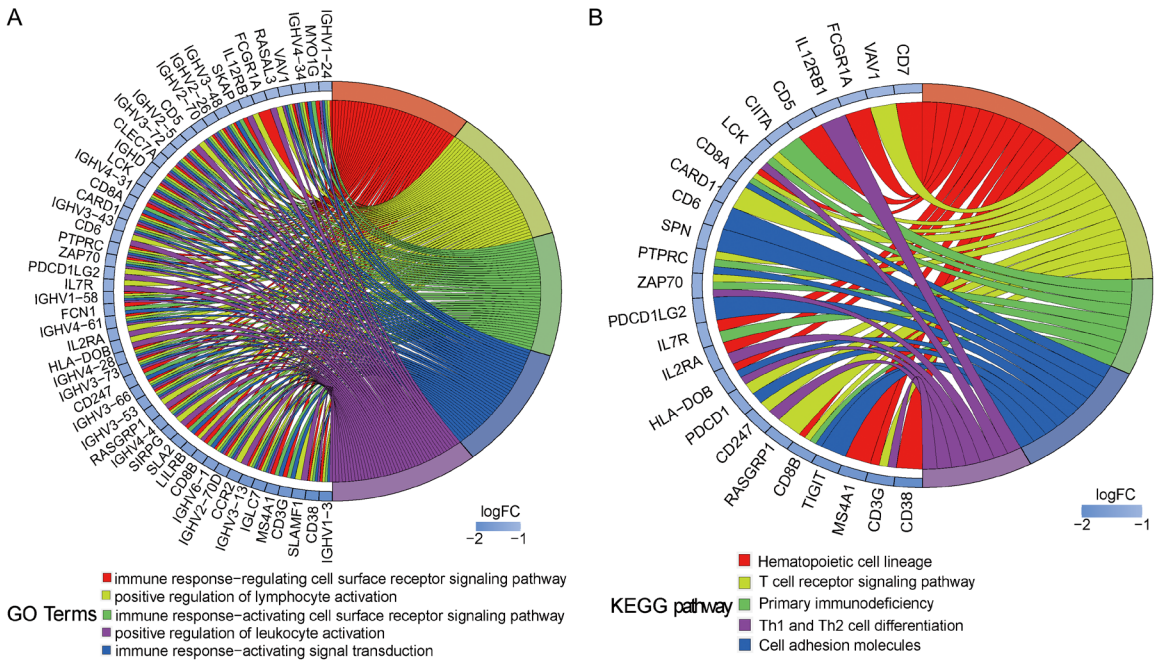

Supplementary Figure 3. The circular diagrams of the differentially expressed genes in two risk subgroups associated with the significant Go term (A) and KEGG pathway (B).

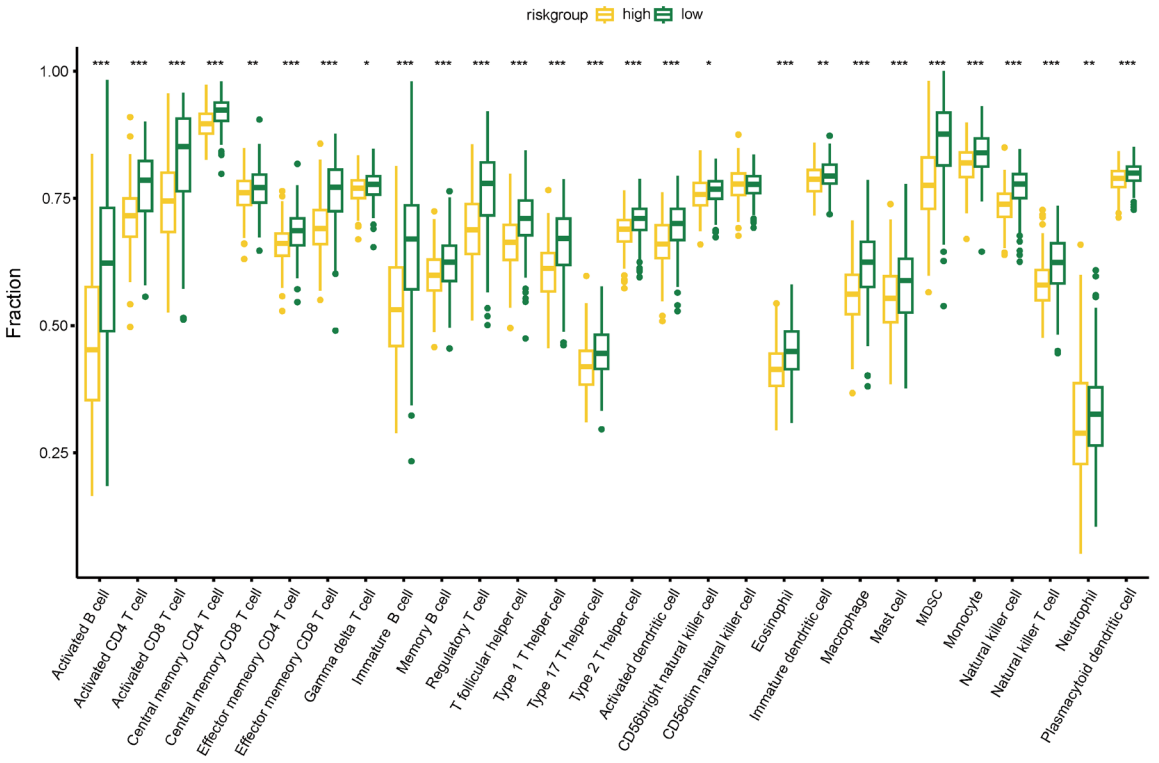

Supplementary Figure 4. Differences in immune cell infiltration between two risk groups by ssGSEA.